High Energy Physics and Nuclear Physics

Volume 21, Number 3

Development and Application of the Fast Monte Carlo Simulation Method for Beijing τ-Charm Factory (BTCF)

Huang Yinzhi, Cheng Baosen, Liu Huaimin, Ma Aimin, Xiong Weijun, Fan Xiaoling, Qi Nading, Zhang Dahua, Chen Shaomin, Xie Yuehong, Li Haibo, Hu Jingliang, and Zhang Jinlong

(Institute of High Energy Physics, The Chinese Academy of Sciences, Beijing, China)

Based on the existing concept design and the expected performance of the detector at the future τ-charm factory, a fast Monte Carlo simulation program using the BES software frame and its data structure has been developed. Various important and/or interesting physics issues have been simulated using this method and a series of important physics results have been attained. The design idea, the program frame, and the advantages of this method have been described. This method can greatly save CPU and disk space and is specially suitable for BES users. The physics results obtained from the simulation demonstrate the physics importance of building the BTCF.

Key words: τ-charm factory, Monte Carlo simulation, *CP* violation, charmonium, $D^0\overline{D}^0$ mixing, spin-parity analysis.

1. INTRODUCTION

The initial idea for a τ-charm factory was proposed by J. Kirkby in 1987, and it has become one of the favorite experiments with a high precision measurement in the high energy physics society; it

Received on October 31, 1996.

keeps attracting physicists from all over the world to study the feasibility of building a τ-charm factory and the physics goals that might be reached with it. In the last ten years, many jobs have been applied to the concept design of τ-charm factory accelerator and detector as well as the Monte Carlo simulation on physics topics. Six international workshops have been held which further promote the progress on the research of τ-charm factory.

In April 1994, we began the Monte Carlo simulation study on τ-charm factory and aimed at probing the feasibility in physics aspects of building BTCF with the collider operating in the center-of-mass energy range 3-5 GeV and a peak luminosity of $1 \times 10^{33}cm^{-2}s^{-1}$. We presented our preliminary results in the 4th τ-charm factory workshop held at SLAC, United States. More results were presented in both the 5th and the 6th τ-charm factory workshops, held respectively at ANL, in the United States in 1995, and at IHEP in China in 1996.

2. FAST MONTE CARLO SIMULATION METHOD

2.1. Design and overall consideration

Due to limited time and computer sources, the following basic idea was maintained throughout the design of the simulation method for the purpose of its easier use by BES collaboration members.

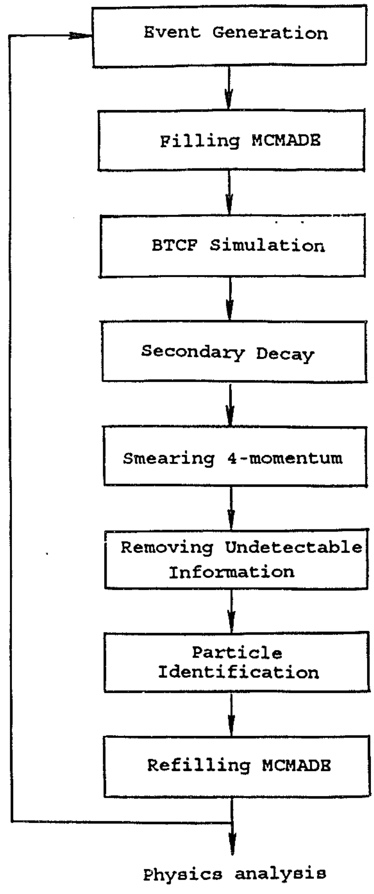

Fig. 1
The flow chart of simulation.

Table 1
The detector parameters of BTCF [1].

Charged particles	
Momentum resolution: σ_p/p(GeV/c)	0.4%p⊕0.4%/β
Angular resolution: σ_ϕ(mrad)	0.5⊕1.1/$p\beta$
$p^{\perp}_{min}(\pi)$ for efficient tracking (MeV/c)	50
Ω (barrel) (×4π sr)	90-95%
Photons	
Energy resolution: σ_E/E(GeV)	2%$E^{1/4}$⊕1%
Angular resolution: $\sigma_{\theta,\phi}$(mrad)	1.7+2$\sqrt{E}$ (at 90°)
2γ angular separation (mrad)	50
E^{γ}_{min} for efficient detection (MeV)	10
Particle identifications	
π-K separation	3σ at 1.0 GeV/c (10^{-3} inc. Cĕ.)
π/K-e separation	0.1%(10^{-5} inc. Cĕ.)
π/K-μ separation	1.5%/p + (1-4%)
K^0_L detection efficiency	95%
n mean detection efficiency	50%
ν detection: $p^{\perp}_{min}$ (MeV/c)	100

First, the event generators, the frame of event simulation program (SOBER) and analysis program (DRUNK), and the data structure (MCMADE) in the BES are kept in use. It greatly decreases the working load of developing codes and makes it easily accessible to BES members. Second, unlike SOBER and DRUNK in BES, the detailed structures of the detector and the particles' behaviors in each subcomponent are ignored. Only the overall parameters such as the resolutions of p, E, θ, and ϕ, the acceptance of θ, E_{min}, and p_{min}, all of which are listed in Table 1, and the particle identification abilities for various particles which are summarized from each relative subdetector, as well as the specific treatment for the particle decay in the detector, are considered in the method. No track finding, reconstructing, and fitting were done. A great amount of manpower and computer sources are spared.

2.2. Flow chart of fast Monte Carlo simulation of BTCF

Figure 1 shows the flow chart of the fast Monte Carlo simulation method. The detailed description is as follows:

(1) Event generation: writing a SOBER card and selecting an event generator in order to produce the required number and type of particles.

(2) Filling the data block: the information generated are stored into the common block MCMADE.

(3) Steering into the BTCF simulation program: the fast Monte Carlo simulation program is called.

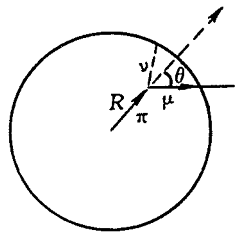

Fig. 2
Secondary decay of particle.

(4) Dealing with the decay case: the particle might decay in the detector (see Fig. 2). The criteria to handle it are:

1. If $R < 5$ cm, keep all secondary particles and discard the primary particle.

2. If $R \geq 5$ cm: (a) if there is no primary charged particle, discard all particles; (b) if there is one secondary charged particle, in case $\theta > 10°$, discard all particles; when $\theta \leq 10°$, keep the secondary particle and discard the primary particle when $R < 35$ cm and treat them in the opposite way when $R \geq 35$ cm; and (c) if there are more than two secondary charged particles, discard all particles.

(5) Smearing of 4-momentum: smear the charged particles' p, θ, and ϕ and the neutral particles' E, θ, and ϕ according to the Gaussian distribution with resolution parameters listed in Table 1.

(6) Remove the undetectable information: the particles along with their information are removed if they are outside the efficient detectable scope according to θ, E_{min}, and p_{min} in Table 1.

(7) Particle identification: three subroutines are called to simulate the particle identification for the different particles — electron, muon, or hadron with the given misidentification rate. For example, from Table 1, 3% π with the momentum of 1 GeV/c will be misidentified as μ.

(8) Refill the data common block: after the above treatment the data are refilled into the data common block. The 4-momentum of particles may change slightly due to the smearing, some particles might be lost or misidentified as others. Certainly, such cases are rare because of the excellent detector performance of BTCF.

When the procedure for this event has been finished, the code will normally return to the next event; however, proceed to the physics analysis if all events required by the card are processed.

The physics analysis is very much similar to that for BES. A DRUNK card and analysis code are needed.

2.3. Usage and check of the parametric simulation

This method employed the same generators, the data structures, and the programs used in the BES for the application of parametric simulation. The process is very similar to that in BES with mainly two cards — SOBER and DRUNK — needed.

The parametric simulation is fast and easily implemented for tuning the parameters of the detector. The latter is especially important for the feasibility study and the R&D, since at these phases the design and the performance of the detector are still being studied and not being able to finalize the tuning of the parameters is inevitable.

This method has been checked with the well-studied events, such as bhabha, dimuon, and $\rho\pi$. The results fit well with that attained by the BES. This proves the reasonable simulation of the electron, muon, hadron, and photon by our parametric method.

3. RESULTS OF PHYSICS SIMULATION BY THE FAST MONTE CARLO METHOD

3.1. τ Physics

3.1.1. Measurement of Michael parameter ρ [2]

In the pure leptonic decay τ, $\tau^- \rightarrow e^- + \bar{\nu}_e + \nu_\tau$, for different V, A types, the standard model predicts different values for Michael parameter ρ in the equation

$$dN / dx = x^2[12(1 - x) - \frac{8}{3}\rho(3 - 4x) + r(x)]$$

Our Monte Carlo simulation shows that only in the center-of-mass energy $\sqrt{s} = 3.55$ GeV, the value of ρ is sensitive over the whole x region; in other energies it is not so. It is just covered by the BTCF energy region. Therefore, the best result can be expected at BTCF.

With 700 hours of running time (about a month) the expected accuracy of ρ will be $\delta\rho/\rho \approx 0.5\%$. This ensures the definite determination of what type the V, A is.

3.1.2. Measurement of m_{ν_τ} upper limit [2]

After all considerations, the energy point has been chosen at 3.68 GeV for this study to suppress the charm quark backgrounds. We selected the channels $\tau \rightarrow KK\pi\nu_\tau$ and $\tau \rightarrow 5\pi\nu_\tau$ as signal channels and

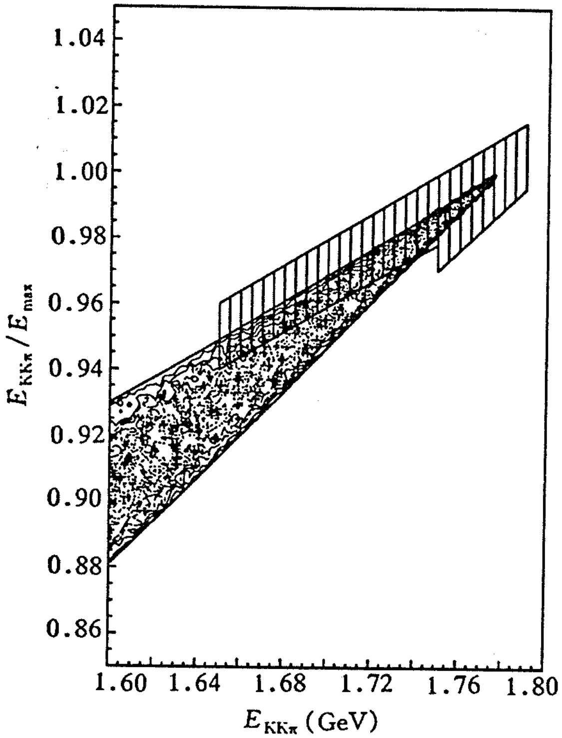

Fig. 3
The sensitive region of two-dimensional fit.

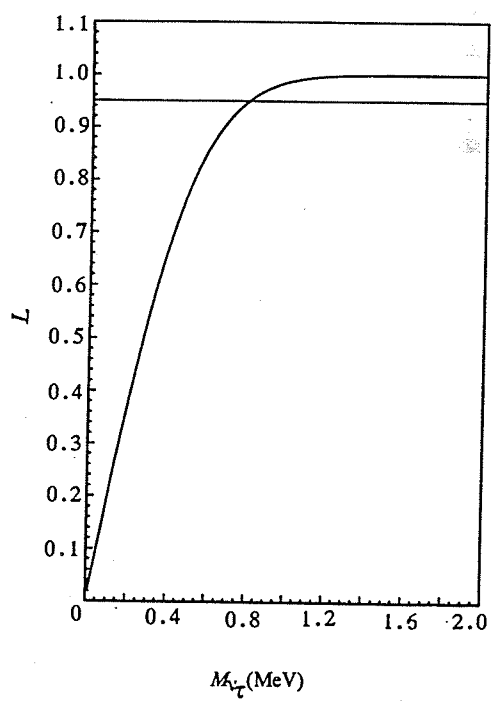

Fig. 4
The likelihood function.

and 6 prongs. The ratio of signal over the background might reach 10^3 with the proper event selection criteria. The sensitive zone, denoted by the vertical line region in Fig. 3, is enlarged with the employment of a 2-dimensional fit, the sensitive fraction of events is $\approx 12\%$ of the total event number (the dark part in Fig. 3), while the usual one-dimensional fit only accounts for the parts with $M_{KK\pi} \geq$ 1.75 GeV. With one year running at BTCF, 1000 $KK\pi\nu_\tau$ events and 160 5 $\pi\nu_\tau$ events can be obtained. Figure 4 gives the likelihood function obtained from these events versus M_{ν_τ}. It shows that the upper limit of M_{ν_τ} is 0.81 MeV (95% C.L.) if only the statistical error considered. With the systematic error (about 0.17 MeV) included, the result of the upper limit less than 1.0 MeV can be expected at BTCF. It will win over the expected result in the B factory.

3.1.3. Study of *CP* violation in τ sector [3]

CP violation in τ sector is one of the most important unsolved problems. The following production-decay sequences are experimentally considered:

$$e^+e^- \to \tau^+\tau^- \to \mu^+\nu_\mu\bar{\nu}_\tau e^- \bar{\nu}_e\nu_\tau$$
$$\to e^+\nu_e\bar{\nu}_\tau \mu^- \bar{\nu}_e\nu_\tau.$$

The amplitude to indicate *CP* violation is defined as

$$A \equiv \langle p_e \cdot (p_{e'} \times p_{\mu'}) \rangle,$$

where p_e, $p_{e'}$, and $p_{\mu'}$ denote the unit momentums of incident electron, electron, and muon decayed from τ.

A is expected to be 0 if no *CP* violation while its value of nonzero indicates *CP* violates [3,4]. A preliminary result with 432 $e\mu$ events at BES gives $A = -0.027 \pm 0.031 \pm 0.006$ where the first error is the statistical and the second the systematic, respectively. With one year running at BTCF the statistical error can be decreased to $\sim 0.05\%$ and the systematic error below 0.1%. *CP* violation in τ sector with the amplitude A about 0.1% can be observed at BTCF.

3.2. Charm physics

3.2.1. Pure leptonic decays of $D_{(s)}$ and the measurement of weak decay constants $f_{D_{(s)}}$ [2]

Pure leptonic decays are the simplest decay modes of $D_{(s)}$. The predicted branching ratios in the standard model are

$$Br(D^+_{(s)} \to l^+\nu_l) = \tau_{D^+_{(s)}} \frac{G_F^2}{8\pi} f^2_{D_{(s)}} M_{D^+_{(s)}} |V_{cd(s)}|^2 M_l^2 \left(1 - \frac{M_l^2}{M^{+2}_{D_{(s)}}}\right)^2,$$

where $D_{(s)}$ denotes D or D_s, $f_{D_{(s)}}$ are the weak decay constants f_D or $f_{D_{(s)}}$ which are important quantities for predicting the other branching ratios of D and D_s, and for understanding the hadron wave function and the second-order weak processes including mixing and *CP* violation. The accuracy of measuring $f_{D_{(s)}}$ depends on the accuracy of the measurements of the pure leptonic branching ratio of $D_{(s)}$ from the above equation. Apart from the high luminosity and the high production rate of $D_{(s)}\bar{D}_{(s)}$, it is of unique advantage at BTCF in the following aspects:

(1) Low background: Almost none of the backgrounds can contribute to the signal according to the distribution of the squared missing mass M^2_{miss} (see Figs. 5 and 6). Furthermore, the backgrounds

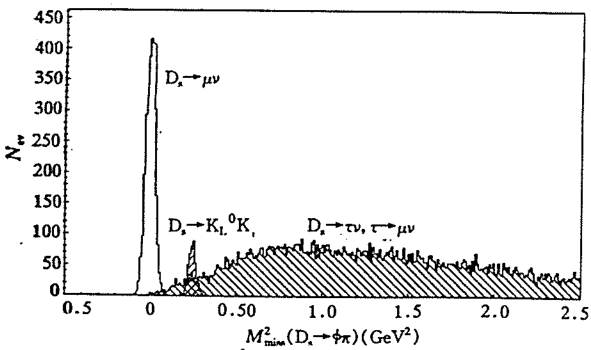

Fig. 5
The squared missing mass of D_s decay.

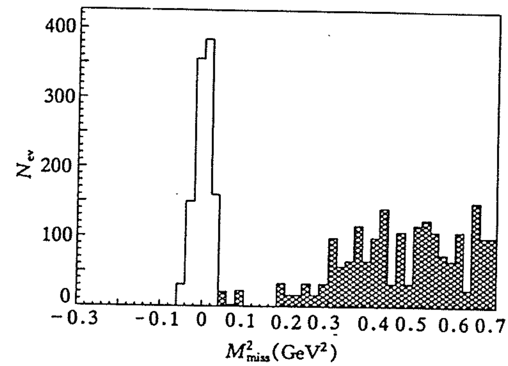

Fig. 6
The squared missing mass of D decay.

can be measured experimentally by lowering the beam energy below the $D_{(s)}\bar{D}_{(s)}$ threshold.

(2) Single-tagging can be applied when running at near the threshold of 3.77 GeV for D and 4.03 GeV for D_s.

(3) The particle identifications are easier due to the kinematic limit of the secondary particles at BTCF.

With one year's data (5000 hrs) at BTCF, $f_{D_{(s)}}$ can be measured to about 2% accuracy including the statistical error and the systematic error.

3.2.2. Study of $D^0\bar{D}^0$ mixing and *CP* violation in charm [5]

$D^0\bar{D}^0$ mixing is closely connected to *CP* violation in neutral D meson decays. Moreover, $D^0\bar{D}^0$ itself is also a good place for testing the standard model and probing new physics beyond it. The mixing rate is experimentally defined as

$$r_D \equiv \frac{N(D^0 \to \bar{D}^0 \to f)}{N(D^0 \to f)} \approx \frac{x^2 + y^2}{2},$$

where $N(D^0 \to \bar{D}^0 \to f)$ is the number of D^0 decaying as $\bar{D}^0$ $N(D^0 \to f)$ is the number of D^0 decaying as D^0, $x \equiv \Delta M/\Gamma$ and $y \equiv \Delta\Gamma/2\Gamma$ come from mixing in the mass and decay matrices, respectively.

Three channels are simulated to study the mixing (see Table 2). An accuracy of better than 10^{-4} can be reached with one year (5000 hrs) running at BTCF as shown in Table 2. Among them the last one has poorer statistics as only one hadron decay channel $D^{\mp} \to K^{\pm}\pi^{\mp}\pi^{\mp}$ is used to tag production of D^0. This can be improved with other hadron decay channels of $D^{\pm}$ added as tag channels.

For *CP* violation induced by $D^0\bar{D}^0$ mixing, the parity *C* of the system is required to be even, i.e., the channel $e^+e^- \to D^0\bar{D}^0\gamma$. The *CP* asymmetry is $2\sqrt{2r_D}A$, where A is defined as

$$A \equiv \frac{N[(K^+e^-\nu)(K^+K^-)] - N[(K^-e^+\nu)(K^+K^-)]}{N[(K^+e^-\nu)(K^+K^-)] + N[(K^-e^+\nu)(K^+K^-)]}.$$

An asymmetry effect of $\sim 1\%$ can be achieved at BTCF which is much worse than the required accuracy to get the value predicted by the present theory.

Table 2
$D^0\bar{D}^0$ mixing.

Reaction	Events	r_D (6 mixing events)	Energy (GeV)
$e^+e^-\to\psi''$, $\psi''\to D^0\bar{D}^0$ $D^0\to K^-\pi^+$, $\bar{D}^0\to K^+\pi^-$	70914	8.5×10^{-5}	3.77
$e^+e^-\to\psi''$, $\psi''\to D^0\bar{D}^0$ $D^0\to K^-e^+\nu$, $\bar{D}^0\to K^+e^-\nu$	60818	9.9×10^{-5}	3.77
$e^+e^-\to D^{*+}D^-$, $D^{*+}\to\pi^+D^0$ $D^0\to K^-e^+\nu$, $D^-\to K^+\pi^-\pi^-$	23171	2.6×10^{-4}	4.03

3.3. Charmonium physics

3.3.1. Study of $\xi(2230)$ neutral decay [2,6]

The result of $\xi(2230)$ given by the BES collaboration group [7] not only confirms the existence of $\xi(2230)$ in the decay channel $J/\psi\to\gamma K\bar{K}$ [8] but also finds two new nonstrange decay modes $\xi\to p\bar{p}$ and $\xi\to\pi^+\pi^-$. The striking features, such as flavor symmetry decay, copious production in radiative J/ψ decay and very narrow partial decay widths to $\pi\pi$ and $K\bar{K}$, strongly favor the glueball interpretation of $\xi(2230)$. However, only 20−40 events are observed for each decay channel of $\xi(2230)$ at BES. It is hard to determine whether the spin of $\xi(2230)$ is 2^{++} or 4^{++}. More channels and more detailed study for the known channels are needed. We simulated 10^8 J/ψ events to study the channel $J/\psi\to\gamma\xi(2230)\to\gamma\pi^0\pi^0$ and got a better result (see Fig. 7).

$\xi(2230)$ is regarded as the candidate of 2^{++} glueball. The lattice gauge theory predicts the mass of 2^{++} glueball to be 2270 ± 100 MeV which is in accordance with that of $\xi(2230)$. We analyzed the spin-parity of $\xi(2230)$. For the convenience of the analysis, the relative background free channel $J/\psi\to\gamma K_s^0K_s^0$ has been chosen and 30,000 such events can be obtained from 10^9 J/ψ data. $2^{++}\xi(2230)$ and $4^{++}\xi(2230)$ are generated for the spin-parity analysis and the maximum likelihood technique has

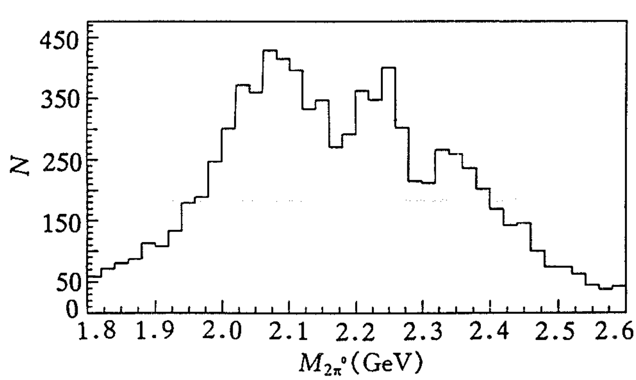

Fig. 7
The invariant mass of $J/\psi\to\gamma\pi^0\pi^0$.

been employed to fit its angular distribution. For 2^{++} data it shows the ratio of the likelihood function for 4^{++} and 2^{++} is

$$L(4^{++}) \,/\, L(2^{++}) = e^{-146} \approx 10^{-61},$$

This indicates clearly that the J^{PC} is 2^{++} but 4^{++}. Figures 8(a) and 8(b) show the $\cos\theta_\gamma$ and $\cos\theta$ distribution after the acceptance correction. The solid line is for 2^{++} while the dashed line for 4^{++}. It also supports $J^{PC} = 2^{++}$. For 4^{++} data the ratio of the likelihood function for 2^{++} and 4^{++} is

$$L(2^{++}) \,/\, L(4^{++}) = e^{-125} \approx 10^{-52},$$

This indicates clearly that the J^{PC} is 4^{++} but 2^{++}. Figures 8(c) and 8(d) show the $\cos\theta_\gamma$ and $\cos\theta$ distribution after the acceptance correction. The solid line is for 4^{++} while the dashed line for 2^{++}. It also supports $J^{PC} = 4^{++}$.

Because of the high luminosity of the BTCF collider and the good performances of the BTCF detector, the conclusion by our Monte Carlo study is that J^{PC} of $\xi(2230)$ can be definitely determined at BTCF whether it is 2^{++} or 4^{++}.

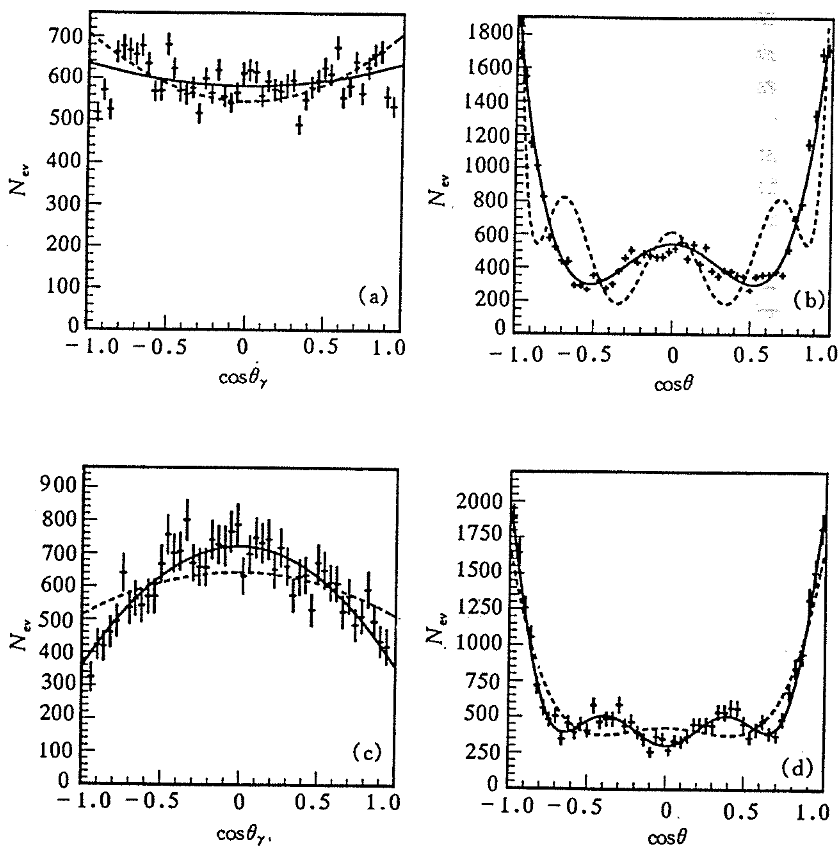

Fig. 8
The spin-parity analysis of $\xi(2230)$.

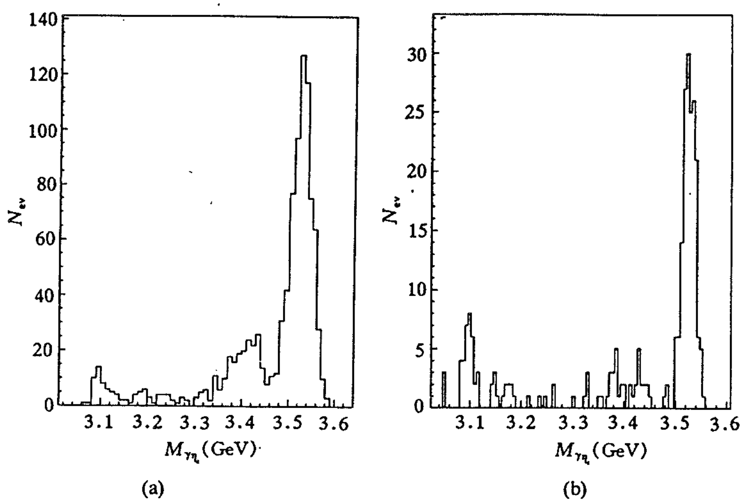

Fig. 9
The invariant mass of $\gamma\eta_c$.
(a) $\gamma\eta_c \to \gamma K^+K^-\pi^0$; (b) $\gamma\eta_c \to \gamma K^+K^-\pi^-$.

3.3.2. Searching for ${}^1P_1$ state and its spin parity analysis

The preliminary results for the mass and the upper limit on the width of ${}^1P_1$ given by the E760 collaboration is the only information for ${}^1P_1$ so far:

$$M({}^1P_1) = 3526.2 \pm 0.15 \pm 0.20\text{MeV},$$
$$\Gamma < 1.1\text{MeV}.$$

The ${}^1P_1$ state can be reached via ψ' decay. A theoretical prediction gives

$$Br(\psi' \to \pi^{0\,1}P_1) = 2 \times 10^{-4},$$
$$Br({}^1P_1 \to \gamma\eta_c) \approx 0.7\,.$$

Two channels, $\psi' \to \pi^0\gamma\eta_c \to \pi^0\gamma K^+K^-\pi^0$ and $\psi' \to \pi^0\gamma\eta_c \to \pi^0\gamma K^+K^-\pi^+\pi^-$, are used to test the ${}^1P_1$ signals. With a 5×10^8 ψ' data sample, a clear ${}^1P_1$ peak can be seen by using some event selection criteria and considering possible backgrounds [see Figs. 9(a) and 9(b)].

The maximum likelihood method is used for the spin-parity analysis of ${}^1P_1$. The events of ${}^1P_1$ with the possible J^P state, e.g., 1^+, 1^-, 2^+, 2^-, and a series of C_0 value are generated for the channel $\psi' \to \pi^0\gamma\eta_c$.

The results show that the theoretical angular distributions of the J^P always fit these data best. As an example, Fig. 10 shows the angular distribution for 1^+ with $C_0 = 5$ data compared with 1^+, 1^-, 2^+, 2^- predictions, respectively. The ratio of the likelihood functions for other J^P states and the generated J^P state is

$$L(J^P_{\text{other}})\,/\,L(J^P_{\text{gen}}) = e^{-50 - -200},$$

From both Fig. 10 and the ratio of L, one can expect to find ${}^1P_1$ state and determine its spin-parity at BTCF.

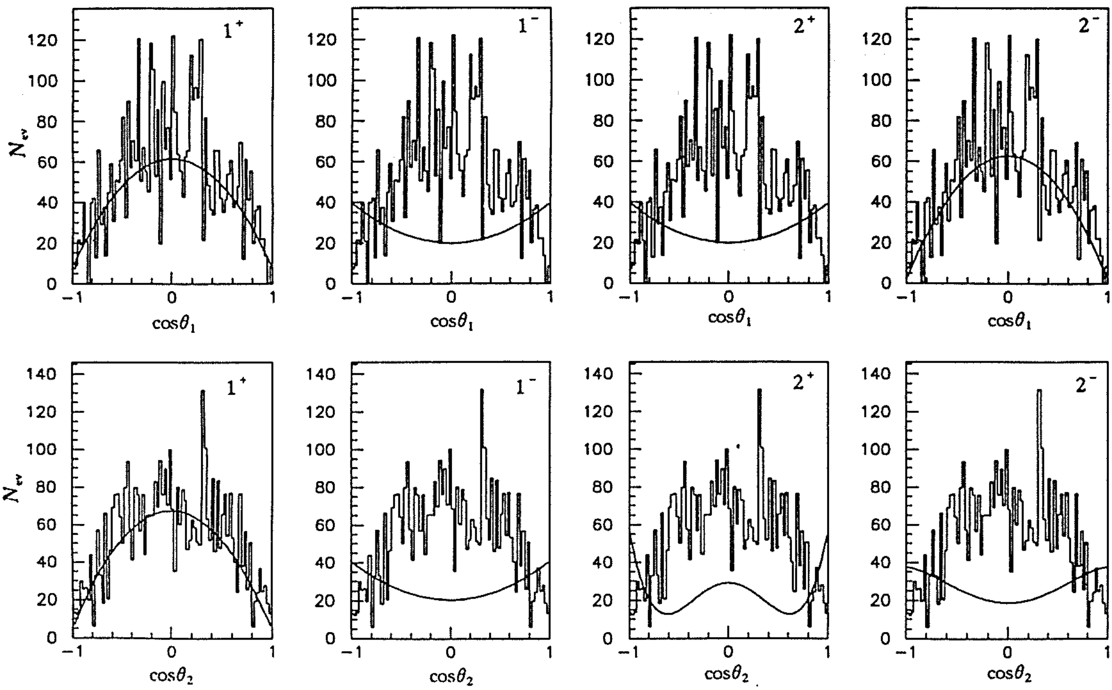

Fig. 10
The spin-parity analysis of $^1P_1$.

4. CONCLUSIONS

A convenient fast Monte Carlo simulation method for BTCF has been developed with the features of saving the computer sources (CPU and disk space) and easily tuning parameters of the detector. Working under the same software environment as the present BES experiment makes it especially suitable for BES collaborators who are the main participants of BTCF. The benefits of this method confirm the successful resolution of a series of important physics issues. They are not only much better than that of present experiments but also superior in the construction of B factories, some of which are even unique at BTCF. It demonstrates the importance to physics of building the BTCF.

ACKNOWLEDGMENTS

We would like to thank Prof. Zheng Zhipeng, Li Jin, Li Weiguo, Gu Yifan, Zhang Changchun, Zhu Yucan, and Zhu Yongsheng for their invaluable assistance. We would also like to thank Prof. Huang Tao, Du Dongsheng, Wu Jimin, and Yu Hong for their effective and pleasant discussions with us. The whole computing environment is supported by the computer center of IHEP, and we give special thanks to them.

REFERENCES

[1] C. Chen *et al.*, *IHEP-BTCF Report-03*, Oct. 1996.
[2] Y.Z. Huang *et al.*, *Proceedings of the Workshop on τ-Charm Factory at IHEP, Feb. 1996, Beijing, China.*

[3] N.D. Qi *et al.*, *Proceedings of 4th International Workshop on Tau Lepton Physics, 16-19 Sept. 1996, Estes Park, CO. USA*.
[4] T.D. Lee, *Proceedings of 17th International Symposium on Lepton-Photon Interaction, 10-15 Aug. 1995, Beijing, China.*
[5] B.S. Cheng, Y.Z. Huang, and A.M. Ma, *Proceedings of the Workshop on τ-Charm Factory at IHEP, Feb. 1996, Beijing, China.*
[6] A.M. Ma, Y.Z. Huang, and B.S. Cheng, *Proceedings of the Workshop on τ-Charm Factory at IHEP, Feb. 1996, Beijing, China.*
[7] J.Z. Bai *et al.* (BES Collaboration), *Phys. Rev. Lett.*, **76**(1996), p. 3502.
[8] R.M. Baltrusaitis *et al.*, *Phys. Rev. Lett.*, **56**(1986), p. 107.